Plasma Jet Braking: Energy Dissipation and Nonadiabatic Electrons

Yu. V. Khotyaintsev,* C. M. Cully, A. Vaivads, and M. André
Swedish Institute of Space Physics, Uppsala, Sweden

C. J. Owen
Mullard Space Science Laboratory, University College London, Dorking, United Kingdom
(Received 8 December 2010; published 18 April 2011)

We report *in situ* observations by the Cluster spacecraft of wave-particle interactions in a magnetic flux pileup region created by a magnetic reconnection outflow jet in Earth's magnetotail. Two distinct regions of wave activity are identified: lower-hybrid drift waves at the front edge and whistler-mode waves inside the pileup region. The whistler-mode waves are locally generated by the electron temperature anisotropy, and provide evidence for ongoing betatron energization caused by magnetic flux pileup. The whistler-mode waves cause fast pitch-angle scattering of electrons and isotropization of the electron distribution, thus making the flow braking process nonadiabatic. The waves strongly affect the electron dynamics and thus play an important role in the energy conversion chain during plasma jet braking.

DOI: 10.1103/PhysRevLett.106.165001 PACS numbers: 52.35.Hr, 52.35.Vd, 94.05.Pt, 94.30.cl

High speed plasma flows, commonly referred to as jets, are ubiquitous in plasma environments. Jets are observed in geospace [1], at the Sun [2], and in various astrophysical objects. Jets always accompany magnetic reconnection, which is one of the key energy conversion processes in magnetized plasmas. The present Letter presents *in situ* observations of these jets in Earth's magnetotail in order to illuminate their dynamics.

A fundamental aspect of jet physics concerns their interaction with the ambient medium and obstacles, which results in braking and dissipation of their bulk flow energy through plasma heating and the production of energetic particles. The flow braking also leads to a pileup of the magnetic field, which is frozen into the plasma. Increasing magnetic field strength in the flux pileup region (FPR) leads to electron betatron acceleration [3,4], with further acceleration possible due to gradient and curvature drifts in electric fields induced during the interaction [5]. Wave-particle interactions may destroy the adiabatic particle motion, leading to irreversible heating. For example, whistler-mode waves are very efficient at scattering electrons in pitch angle [6]. Recent observations in the magnetotail have shown that FPR fronts are narrow regions with a typical transverse size of several ion inertial lengths $c/\omega_{\rm pi}$, with large changes in magnetic field, density and temperature, and associated strong electromagnetic and electrostatic emissions in a broad frequency range [4,7–10]. Here we present detailed observations of wave-particle interactions in the FPR and show that the waves play an important role in energy dissipation in fast plasma jets.

We analyze Cluster [11] observations on September 3, 2006, of a fast plasma flow produced at a magnetic reconnection site in Earth's magnetotail; some aspects of this event have previously been reported by Asano *et al.* [4]. The Cluster satellites were located at $[-15, -3, 1]$ Earth radii (R_E) in Geocentric Solar Magnetospheric (GSM) coordinates and were initially in the central plasma sheet where they detected a fast Earthward plasma flow reaching a maximum speed above 800 km/s at 21:56:35 UT [Fig. 1(b)]. Prior to the flow maximum, a sharp B_z increase [Fig. 1(c)] and an associated sharp increase in the electron energy to >100 keV [Fig. 1(a)] is observed. By comparing observation times at all four Cluster spacecraft (the spacecraft configuration is shown in Fig. 2(a)], the speed of the B_z structure was determined as $V = 450 * [0.91, 0.41, 0.08]$ km/s GSM. Although similarly Earthward-propagating, the B_z structure moves more slowly than the ion jet. The FPR is identified between the B_z peak and the flow maximum [marked by an arrow in Fig. 1(b)]; the plasma flow velocity increases and the magnetic field decreases in the FPR, consistent with plasma flow braking and magnetic flux pileup.

The FPR is associated with strong wave activity in both the electric and magnetic fields. Strong electric fields up to 60 mV/m and electrostatic wave activity covering the lower-hybrid (LH) frequency range [Fig. 1(g)], $f_{\rm LH} \sim 5$–15 Hz, are observed at the front (21:56:20 UT) and rear (21:56:35 UT) edges of the FPR. The LH-waves are localized at the magnetic field and density (not shown) gradients, which have transverse scale ~500 km, $\sim c/\omega_{\rm pi}$ (deduced from the multi-SC timing). There is also a temperature anisotropy with $T_\perp/T_{||} < 1$ [Fig. 1(d), Fig. 3(a)] related to the LH-waves.

Behind the B_z peak (inside the FPR), the sign of the electron anisotropy [Fig. 1(d), Fig. 3(b)] changes to $T_\perp/T_{||} > 1$ for energies above ~3 keV, with the anisotropy extending up to energies above 100 keV. Electromagnetic waves at frequencies ~100 Hz are observed in this region [Fig. 1(e) and 1(f)]. The waves are

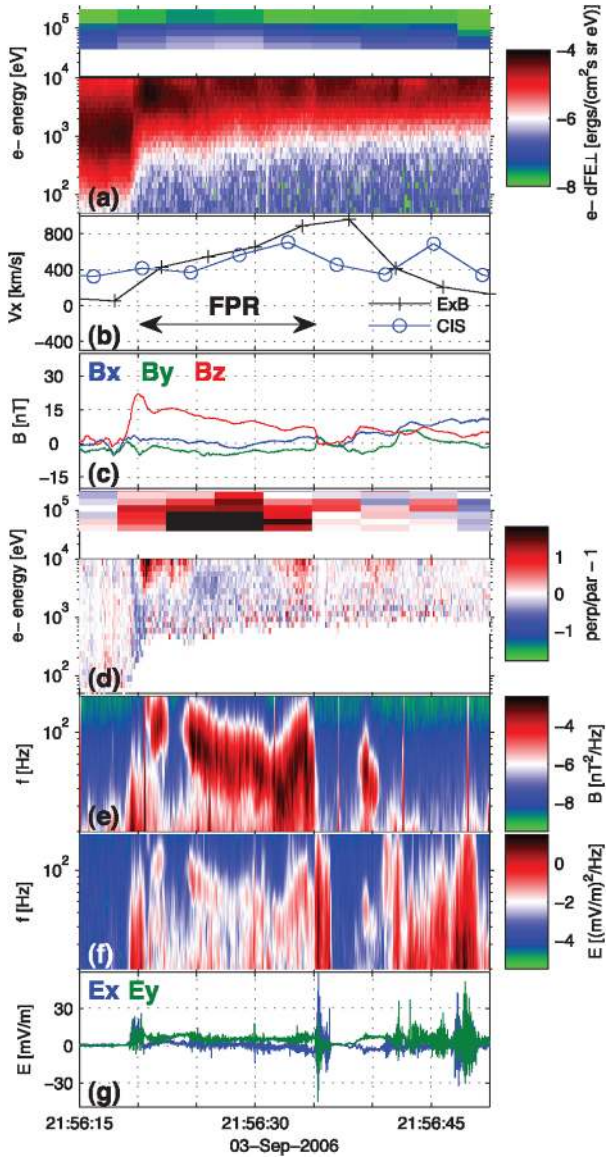

FIG. 1 (color online). FPR observed by Cluster C1. (a) the electron flux from the Research with Adaptive Particle Imaging Detectors (RAPID, >30 keV) and Plasma Electron and Current Experiment (PEACE, <10 keV). (b) GSM X component of the ion flow from the Hot Ion Analyzer (HIA) of the Cluster Ion Spectrometry (CIS) experiment and $E \times B$ from the Electric Field and Wave (EFW) and fluxgate magnetometer (FGM) experiments. (c) Magnetic field GSM components from FGM. (d) Electron flux anisotropy, with zero corresponding to isotropic fluxes; fluxes below 10^{-6} ergs/(cm^2 s sr eV) are excluded below 10 keV. (e) Magnetic field spectrum (20–180 Hz) from the Spatio Temporal Analysis of Field Fluctuations (STAFF) experiment. (f) Electric field spectrum and (g) waveform.

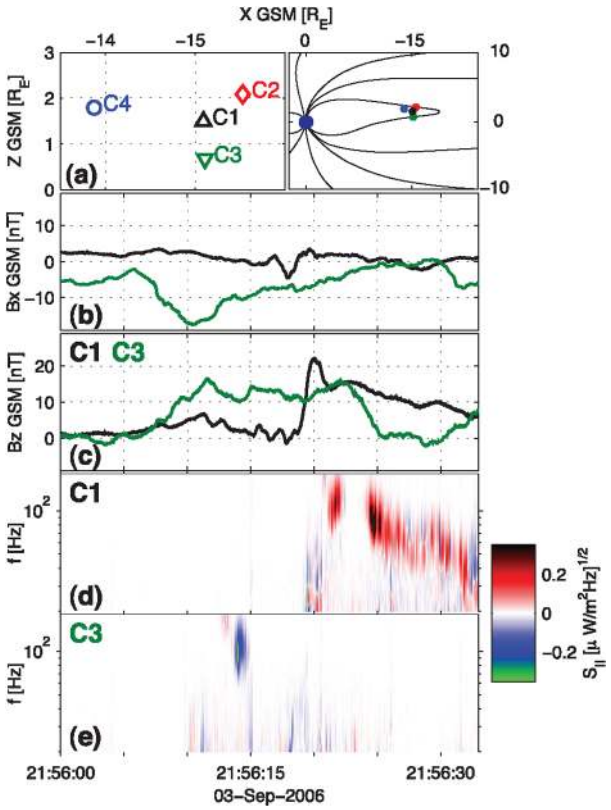

FIG. 2 (color online). Multispacecraft observations of whistler-mode waves. (a) Location of the Cluster SC in the XZ GSM plane: detail of cluster tetrahedron (left) and position relative to the magnetotail current sheet (right). (b) and (c) C1 and C3 observations of B_x and B_z GSM, respectively. The two bottom panels show the parallel component of the Poynting flux in the frequency range 20–180 Hz for C1 (d) and C3 (e).

circularly right-hand polarized and propagate close to the direction of the magnetic field (within 20° as determined by minimum variance analysis of δB). The waves are relatively narrow-band, and the wave frequency follows approximately one quarter of the local electron gyrofrequency, $f_{ce}/4$. This suggests that these waves are whistler-mode waves. The waves have amplitudes up to 0.5 nT and 5 mV/m. The phase velocity given by the $\delta E/\delta B$ ratio is $\sim 10^4$ km/s. Similar whistler-mode waves and electron anisotropy are observed at C3 and C4.

Figure 2 shows data from Cluster C1 and C3, which are at similar locations along the plasma flow direction (X GSM) and are separated by $\sim$5000 km in Z GSM, i.e., in the direction perpendicular to the flow and the magnetotail current sheet [Fig. 2(a)]. C3 is located below the current sheet ($B_x < 0$) and C1 is slightly above the current sheet ($B_x \geq 0$). The B_z increase is seen first by C3 and then by C1, consistent with the Earthward motion of the B_z front [Fig. 2(c)]. Figures 2(d) and 2(e) show the field-aligned Poynting flux at C1 and C3; the same structure at $\sim$100 Hz is observed in a local minimum of B_z following the peak at 21:56:14 UT at C3 and at 21:56:21 UT at C1. The wave structures have the same time delay as the B_z front, suggesting that the structures are generated by the same spatial source propagating with the front. Moreover, the Poynting flux is positive on C1 and negative on C3, indicating that the generation region is located between the spacecraft, i.e., close to the current sheet center. This is confirmed by

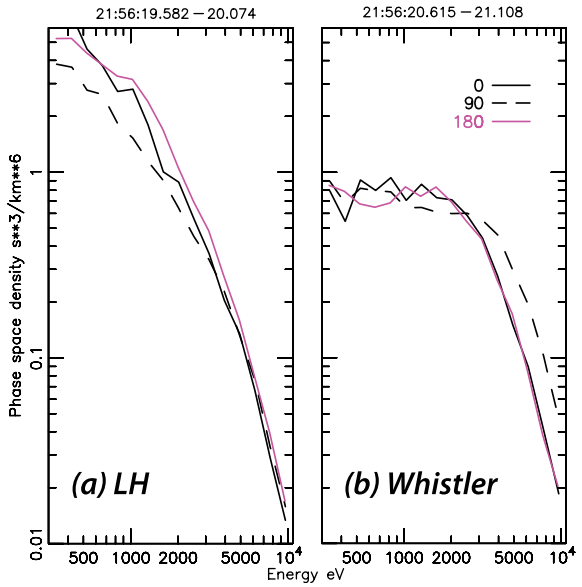

FIG. 3 (color online). Examples of observed electron distribution functions. (a) Parallel flux dominates over perpendicular flux at the front edge of the FPR, associated with LHD waves. (b) Nearby in the FPR in association with whistler-mode waves, the distribution is flat-top at low energies and dominated by perpendicular flux at higher energies.

C1 detecting bidirectional Poynting flux when located in the current sheet center ($B_x \sim 0$, 21:56:27–33 UT). The observed location of the generation region is similar to that of whistler-mode chorus waves: close to the geomagnetic equator, where the magnetic field magnitude is smallest along the fieldline [12].

Figure 3 shows the different types of electron distributions observed in the FPR. At the front edge of the FPR, the distribution is approximately bi-Maxwellian with $T_\perp/T_{||} < 1$ [Fig. 3(a)]. The front edge is a narrow structure $\sim c/\omega_{\rm pi}$, with strong gradients in both B and plasma density, and is reminiscent of the separatrix region at the magnetopause [13]. Strong waves in the LH range are observed, and we suggest that these are drift LH-waves driven by the gradients. Similar observations of LH waves have been reported from the THEMIS spacecraft [8]. LH waves lead to electron heating in the parallel direction [14], which is consistent with the observed anisotropy [Fig. 3(a)].

The opposite anisotropy, $T_\perp/T_{||} > 1$, is observed just 0.5 s later [Fig. 3(b)] and throughout the FPR. The perpendicular flux exceeds the parallel at energies above 2 keV. This is likely due to increasing magnetic field during the flux pileup causing electron betatron acceleration. At these energies, the distribution has nearly constant phase space density along the whistler-mode quasilinear diffusion curves, consistent with marginal stability [15]. We posit that the distribution was previously unstable and has relaxed to this whistler-mode-stable state. Using the observed parameters from C1 at 21:56:21 UT, the quasilinear pitch-angle diffusion rate [16] exceeds 1 s^{-1} for electrons with parallel energies between 2 and 8 keV, with maximum diffusion rates near 50 s^{-1}. The observed whistler-mode waves can therefore modify the electron distribution on the time scale of seconds. As the magnetic field increases, betatron acceleration forces the particles to larger perpendicular energies. However, the anisotropy is eventually limited by the whistler-mode interaction, which predominantly scatters the electrons back to smaller pitch angles. At higher (100 keV) energies, the wave-particle interaction is only efficient near 90° pitch angles, so the anisotropy in that range may exceed the whistler-mode marginal stability threshold (as observed) without driving strong wave-particle interactions.

The wave-particle interaction breaks the first adiabatic invariant, resulting in irreversible heating, and the wave power generated during this whistler-limited betatron acceleration carries energy away from the current sheet. This process is reminiscent of magnetic pumping used to heat plasma in laboratory devices, where the scattering is due to regular Coulomb collisions [17]. At some distant point the wave energy may again be transferred back into heating or electron acceleration [18].

Below 2 keV, the overall shape of the distribution in Fig. 3(b) is a so-called "flat-top", with constant phase space density over a broad energy range. Such distributions are characteristic of the reconnection diffusion region [19]. We propose the following scenario for formation of the flat-top distribution. When the electron beam is ejected from the diffusion region at approximately the electron Alfvén speed $V_{\rm Ae}$, it eventually encounters a region with stronger magnetic fields and evolves into a "shell" distribution, which is unstable to generation of whistler-mode waves. These waves rapidly flatten the inside part of the shell to form the observed flat-top distribution. In this scenario the flat-top energy ~2 keV approximately corresponds to the energy of the source electron beam, $m_e V_{\rm Ae}^2/2$, which agrees with typical $V_{\rm Ae}$ values in the magnetotail diffusion region.

The boundary at which the character of the electron distribution (sign of the temperature anisotropy) changes is very sharp; the two distributions in Fig. 3 are just 0.5 sec (200 km) apart. No significant electric fields are observed at this location to make such a dramatic change in the distribution function. Therefore this boundary is most likely tangential; i.e., there is no plasma transport across the boundary. In such a case, all the plasma behind the boundary comes from the reconnection X-line, which is consistent with our proposed generation scenario for the observed flat-top distributions.

We have presented detailed observations of waves and electron distributions in a region associated with plasma flow braking and magnetic flux pileup in Earth's magnetotail. Our findings can be summarized as follows: 1. Inside the flux pileup region (FPR) we observe whistler-mode

waves and an anisotropic distribution $T_\perp/T_{||} > 1$. We show that the waves are locally generated close to the center of the current sheet where the magnetic field is the smallest. Consistent with betatron heating due to the magnetic flux pileup, the whistler-mode waves are driven by the anisotropy of the electron distribution function (the observed distribution is marginally stable), and hence offer a marker for betatron acceleration. We conclude that betatron acceleration occurs locally within the FPR. 2. The observed whistler-mode waves have sufficient amplitude to cause strong pitch-angle scattering of electrons, thus making the betatron acceleration nonadiabatic (irreversible). 3. Whistler-mode wave-particle interaction limits the electron anisotropy caused during the betatron acceleration process at lower energies. The resulting distribution has limited anisotropy below 2 keV, and is more anisotropic at higher energies. 4. Strong lower-hybrid drift (LHD) waves are observed at the front edge of the plasma jet, where the magnetic field strength increases steeply over a scale $\sim c/\omega_{\mathrm{pi}}$. The electron distribution observed simultaneously with the LHD waves is anisotropic with $T_\perp/T_{||} < 1$ at energies starting from 100 eV, which is consistent with heating by LHD waves. 5. Evolution of the electron distribution function indicates that the boundary between the front edge ($T_\perp/T_{||} < 1$) and the downstream FPR ($T_\perp/T_{||} > 1$) is tangential; i.e., all the electrons in the FPR come from the downstream region, and never encounter the dipolarization front. The data suggest that the most energetic electrons are located inside the FPR, which indicates that most acceleration happens there and not at the front.

Our observations show that wave generation strongly affects the electron dynamics, and plays a crucial role in the energy conversion chain during plasma jet braking. The results presented must be of universal importance for solar and astrophysical environments.

We thank the Cluster Active Archive for providing the data for this study. The research of Y. K., C. C., and A. V. is supported by the Swedish Research Council, grants 2007-4377, 2009-3957, and 2009-4165. We also acknowledge support from ISSI.

*yuri@irfu.se

[1] V. Angelopoulos *et al.*, J. Geophys. Res. **97**, 4027 (1992).
[2] S. Masuda, T. Kosugi, H. Hara, S. Tsuneta, and Y. Ogawara, Nature (London) **371**, 495 (1994).
[3] J. Birn, M. F. Thomsen, and M. Hesse, Phys. Plasmas **11**, 1825 (2004).
[4] Y. Asano *et al.*, J. Geophys. Res. **115**, 5215 (2010).
[5] M. Hoshino, J. Geophys. Res. **110**, 10 215 (2005).
[6] R. M. Thorne, B. Ni, X. Tao, R. B. Horne, and N. P. Meredith, Nature (London) **467**, 943 (2010).
[7] A. Runov *et al.*, Geophys. Res. Lett. **36**, 14 106 (2009).
[8] V. Sergeev *et al.*, Geophys. Res. Lett. **36**, 21 105 (2009).
[9] O. Le Contel *et al.*, Ann. Geophys. **27**, 2259 (2009).
[10] X. Deng *et al.*, J. Geophys. Res. **115**, 9225 (2010).
[11] *The Cluster and PHOENIX missions*, edited by C. P. Escoubet, C. T. Russell, and R. Schmidt (Kluwer, Dordrecht, 1997).
[12] O. Santolík, D. Gurnett, and J. Pickett, Ann. Geophys. **22**, 2555 (2004).
[13] Y. V. Khotyaintsev, A. Vaivads, A. Retinò, M. André, C. J. Owen, and H. Nilsson, Phys. Rev. Lett. **97**, 205003 (2006).
[14] I. H. Cairns and B. F. McMillan, Phys. Plasmas **12**, 102110 (2005).
[15] R. Gendrin, Rev. Geophys. **19**, 171 (1981).
[16] L. Lyons, J. Plasma Phys. **12**, 417 (1974).
[17] J. M. Berger, W. A. Newcomb, J. M. Dawson, E. A. Frieman, R. M. Kulsrud, and A. Lenard, Phys. Fluids **1**, 301 (1958).
[18] R. B. Horne and R. M. Thorne, Geophys. Res. Lett. **25**, 3011 (1998).
[19] Y. Asano *et al.*, J. Geophys. Res. **113**, 1207 (2008).